Broadening of the superconducting transition by fluctuations in three-dimensional metals at high magnetic fields

T. Maniv,[1] V. Zhuravlev,[1] J. Wosnitza,[2,3] O. Ignatchik,[2,3] B. Bergk,[3] and P. C. Canfield[4]
[1]*Chemistry Department, Technion–Israel Institute of Technology, Haifa 32000, Israel*
[2]*Hochfeld-Magnetlabor Dresden (HLD), Forschungszentrum Rossendorf, D-01314 Dresden, Germany*
[3]*Institut für Festkörperphysik, Technische Universität Dresden, D-01062 Dresden, Germany*
[4]*Ames Laboratory and Department of Physics and Astronomy, Iowa State University, Ames, Iowa 50011, USA*
(Received 25 February 2005; revised manuscript received 24 January 2006; published 27 April 2006)

The Bragg-chain model of the two-dimensional (2D) vortex state at high magnetic field [V. N. Zhuravlev and T. Maniv, Phys. Rev. B **60**, 4277 (1999)] is extended to an array of coupled superconducting (SC) layers. Application to MgB_2 and YNi_2B_2C yields good quantitative agreement with high-field magnetization measurements, indicating that the smeared transitions observed in these materials are, at least in great part, due to SC fluctuations. Similar to the situation in a 2D system, the melting of the vortex lattice in strongly coupled SC layers is predicted to occur well below the mean field H_{c2}.

DOI: 10.1103/PhysRevB.73.134521 PACS number(s): 74.40.+k, 74.25.Ha, 74.70.Ad, 74.70.Dd

It is well known that the transition from the normal to the superconducting (SC) state in type-II three-dimensional (3D) superconductors in the absence of an external magnetic field is a sharp, second-order phase transition, with a vanishing order parameter at the transition temperature T_c. Fluctuation effects can smear the transition significantly in high-T_c and low-dimensional superconductors,[1–3] where the phase space accessible for the fluctuations is dramatically enhanced. The influence of an external magnetic field is similar to an effective reduction of dimensionality[4] resulting in a significant smearing of the transition even at very low temperatures. Such strong smearing effects have been observed in various quasi-two-dimensional (2D) low-T_c superconductors at high magnetic fields.[5–7]

In conventional 3D superconductors one usually expects much weaker smearing effects at high magnetic fields, though there is no sharp phase transition at any temperature $T>0$ also in this case (for which the effective dimensionality of the fluctuations is $D=1$). Fluctuation effects in the limiting cases of 2D and 3D superconductors at high magnetic fields have been studied extensively by Tesanovic and co-workers,[8] and more recently by Li and Rosenstein,[9–11] who focused on analyzing thermodynamic scaling functions in the large critical region characterizing high-T_c superconductors.

In the present paper we extend our theory of the 2D vortex state in strongly type-II superconductors at high magnetic fields[12,13] to an array of coupled SC layers, and investigate the influence of the interlayer coupling on the SC transition in the entire 2D-3D crossover region. It is shown theoretically, and confirmed experimentally, that thermal fluctuations strongly affect the SC transition in conventional 3D superconductors at high magnetic fields, yielding essentially the same transition width as observed in quasi-2D superconductors such as the organics.[6,7] Similar to the situation in a 2D superconductor, the melting of the vortex lattice in strongly coupled SC layers should take place well below the mean field (MF) $H_{c2}(T)$.

These results, indeed, provide a firm support for the idea raised in Refs. 14 and 15, that the broad transition to the SC state, observed recently in de Haas–van Alphen (dHvA) measurements on MgB_2, is at least in great part due to SC thermal fluctuations. Further support for the importance of thermal-fluctuation effects on the SC transition in conventional 3D superconductors is provided by our magnetization measurements, carried out on YNi_2B_2C single crystals. Our analysis of the observed oscillatory, as well as the steady torque signals, which exhibit a considerably broadened SC transition, yields good quantitative agreement between theory and experiment.

The calculation is carried out by extending the Bragg-chain model of the 2D vortex state at high perpendicular magnetic field[12,13] to an array of strongly coupled 2D SC layers. The validity of this model in the entire normal SC (NSC) crossover region investigated is justified by comparing our result for the SC free energy in the 2D model with the exact high- and low-temperature asymptotic expansions obtained in Ref. 10. Very good quantitative agreement has been found in both limits.

We start with the microscopic BCS Hamiltonian for electrons in a layered 3D metal, interacting via an effective two-body attractive potential under the influence of a strong static magnetic field. We assume, for simplicity, that the magnetic-field direction (along the z axis) is perpendicular to the layers situated parallel to the (x,y) plane. Writing down the functional integral expression for the partition function of this system, the electronic field can be eliminated by introducing the bosonic complex field $\Delta(\mathbf{r})$ (by means of the Hubbard-Stratonovich transformations), which describes all possible realizations of Cooper-pair condensates.[8,13] Expansion of the resulting free-energy functional $F_G[\Delta(\mathbf{r})]$ in the order parameter up to the quartic term is a good approximation for magnetic fields around the MF H_{c2}.

In the lowest Landau-level approximation, which is valid at high magnetic fields and low temperatures,[8] the most general form of the order parameter $\Delta(\mathbf{r})$ is a coherent superposition of Landau wave functions $\phi_q(x,y)=\exp[iqx-(y/a_H+qa_H/2)^2]$:

$$\Delta(x,y,z)=\sum_{n,m} c_q(z)\phi_q(x,y), \tag{1}$$

where $c_q(z)$ are arbitrary complex functions of the coordinate z, defined on the quasi-continuous lattice $q=(2\pi/a_x a_H)(n+m/\sqrt{N})$, with $n,m=-\sqrt{N}/2+1,\ldots,\sqrt{N}/2$, which determines the projections of the orbital guiding centers on the y axis. Here N is the total number of flux lines threading the SC sample, and $a_H=\sqrt{c\hbar/eH}$ is the magnetic length.

In the common approach to this problem, which was first employed by Ruggeri and Thouless,[16] and further developed by Hikami *et al.*,[17,18] Wilkin and Moore,[19] and more recently by Li and Rosenstein,[10] one constructs a high-temperature perturbation expansion including all the Landau modes described above. The expansion is in the quartic coupling constant of the Ginzburg-Landau (GL) theory, and a Feynman diagram technique with various resummation methods which enable the extrapolation of the resulting free energy into the desired low-temperature region. However, all extrapolation attempts made so far within this approach have failed to yield the Abrikosov vortex-lattice state, predicted by the MF theory.

As discussed in detail in Ref. 20, the quasicontinuous, smoothly distributed basis functions, such as those considered by the above mentioned works, cost a very large fraction of the total SC condensation energy and should be drastically "suppressed" in order to yield the expected vortex-liquid freezing transition well below the MF H_{c2}. This can be achieved by rearranging the "continuously" distributed N Landau basis functions in Eq. (1) into a discrete series of weakly overlapping, macroscopically ($\sim\sqrt{N}$) occupied, $\sqrt{N}$ Landau orbitals $\phi_{q_n}(x,y)$ with $q_n=[2\pi/(a_x a_H)]n$ and $n=0,\pm1,\pm2,\ldots$, which ensures the recovery of the vortex-lattice state at low temperatures within low-order perturbation theory.

Surprisingly enough, this discrete-chain approximation, which yields good quantitative agreement with the low-temperature perturbation expansion, presented in Ref. 10, remains a good approximation also in the high-temperature region (see below). Indeed, including any contributions from the interstitial modes, neglected in the Bragg-chain model, would always increase the fluctuation effect, so that near and above the MF transition the fluctuation effect, calculated in this model, should always underestimate the actual effect. However, the error is quite small, as shown in Ref. 21, where the discrete-chain approximation for the generalized Abrikosov parameter yields good quantitative agreement with the numerical simulations of Kato and Nagaosa.[22]

Thus, writing $c_{q_n}(z)\equiv c_n(z)=|c_n(z)|e^{i\varphi_n(z)}$, the phase $\varphi_n(z)$ determines the relative lateral position $x_n=-\varphi_n/q_n$ of the nth Landau orbital within a single 2D layer. It was shown in Ref. 20 that by selecting the x direction along the main principal crystallographic axis of the 2D Abrikosov vortex lattice, the variables $\xi_n\equiv\varphi_n-\varphi_{n-1}$ describe the lateral positions of the most easily sliding vortex chains in the vortex lattice, which are generated mainly by interference between two neighboring Landau orbitals.

The corresponding free-energy functional, projected on the subspace of the lowest Landau level, can be written in a local anisotropic GL form[13,23]

$$F_{\mathrm{GL}}=\int\frac{d^3r}{v}\left[-\alpha|\Delta(\mathbf{r})|^2+\frac{\beta}{2}|\Delta(\mathbf{r})|^4+\gamma\left|\frac{\partial\Delta(\mathbf{r})}{\partial z}\right|^2\right], \tag{2}$$

where $v=\pi a_H^2 d$ is the volume of a single vortex per layer and the effective GL coefficients α, β, and γ can be expressed in terms of the microscopic normal electron parameters (see below). It is convenient to divide the length L_z of the sample perpendicular to the layers into N_z segments of length d, $L_z=N_z d$, where d is the interlayer distance, and to define a discrete set $c_{n,\zeta}=|c_{n,\zeta}|e^{i\varphi_{n,\zeta}}\equiv c_n(z_\zeta)$, with $\zeta=1,2,\ldots,N_z$ and the periodic boundary conditions $c_{n,N_z+1}=c_{n,1}$.

Using Eq. (1), the partition function can be written as

$$\mathcal{Z}\equiv\mathcal{Z}_{ch}^{\sqrt{N}}=\int D\Delta(\mathbf{r})D\Delta^{\star}(\mathbf{r})\exp\{-F_{\mathrm{GL}}[\Delta(\mathbf{r})]/k_BT\},$$

where $\mathcal{Z}_{ch}$ is evaluated as a multiple integral $\Pi_{n,\zeta}\int|c_{n,\zeta}|d|c_{n,\zeta}|\int d\varphi_{n,\zeta}e^{-F_{\mathrm{GL}}/(\sqrt{N}k_BT)}$, with

$$\begin{aligned}\frac{F_{\mathrm{GL}}}{(a_x/\sqrt{2\pi})\sqrt{N}}=&-\alpha\sum_{n,\zeta}|c_{n,\zeta}|^2+\eta\sum_{n,\zeta}|c_{n,\zeta+1}-c_{n,\zeta}|^2\\&+\frac{\beta}{2^{3/2}}\sum_{n,s,p;\zeta}\lambda^{s^2+p^2}|c_{n,\zeta}||c_{n+s+p,\zeta}||c_{n+s,\zeta}||c_{n+p,\zeta}|\\&\times e^{i(\varphi_{n+s,\zeta}+\varphi_{n+p,\zeta}-\varphi_{n,\zeta}-\varphi_{n+s+p,\zeta})}\end{aligned} \tag{3}$$

and $\eta=d^2\gamma$. In this Landau-orbital representation of the GL functional, Eq. (2), the off-diagonal elements constitute a rapidly convergent series in the small expansion parameter $\lambda\equiv e^{-(\pi/a_x)^2}\approx0.066$. Neglecting all terms of order higher than the second, the GL functional takes the form

$$\begin{aligned}\frac{F_{\mathrm{GL}}}{\frac{a_x}{\sqrt{2\pi}}\sqrt{N}}=\sum_{n,\zeta}\Bigg[&-\alpha|c_{n,\zeta}|^2+\eta|c_{n,\zeta+1}-c_{n,\zeta}|^2\\&+\frac{\beta}{2^{3/2}}(|c_{n,\zeta}|^4+4\lambda|c_{n,\zeta}|^2|c_{n+1,\zeta}|^2\\&+4\lambda^2|c_{n,\zeta}|^2|c_{n+1,\zeta}||c_{n-1,\zeta}|\cos\chi_{n,\zeta})\Bigg],\end{aligned} \tag{4}$$

where $\chi_{n,\zeta}\equiv(\varphi_{n+1,\zeta}+\varphi_{n-1,\zeta}-2\varphi_{n,\zeta})$.

In the 2D limit of Eq. (4), where $\eta\to0$, the effective free energy can be evaluated quite accurately in both the low- and high-temperature limits. This can be done in terms of a single dimensionless scaling parameter, given essentially by the ratio between the SC condensation energy (per vortex) and the thermal energy, i.e., $\varepsilon=\alpha^2/(2\beta k_BT)$, which is large in both limits. At high temperatures one may neglect the contributions from both the phase fluctuations ($\sim\lambda^2$) and the amplitude fluctuations involving nearest-neighbor interchain interactions ($\sim\lambda$). Then, one can calculate the partition function with reduced GL energy [including only diagonal terms in Eq. (4)]. The resulting effective free energy (normalized as in Ref. 10) is given by the asymptotic expansion

$$f_{\rm eff} \sim \ln \varepsilon + \frac{1}{\varepsilon} - \frac{5}{4\varepsilon^2} + \cdots,$$

which is only slightly different from the optimized perturbation expansion $f_{\rm eff}^{\rm opt} \sim \ln \varepsilon + (1/\varepsilon) - (1/\varepsilon^2) + \cdots$, derived in Ref. 10.

It is more interesting to compare the discrete-chain model with the optimized perturbation theory at low temperature, where the contribution of phase fluctuations is dominant. Fortunately, this contribution can be calculated exactly, as shown in Ref. 12. Furthermore, calculating the contribution from amplitude fluctuations with the same accuracy as done in the high-temperature limit, we find that

$$f_{\rm eff} \sim -\frac{2\varepsilon}{\beta_A} + \ln \varepsilon - \frac{c}{\varepsilon} + \cdots,$$

with $c \approx 1/(16\pi\lambda^2) \approx 4.7$. Thus, in our expression the first two terms coincide with the optimized perturbation series obtained in Ref. 10, whereas our third term should be compared with $c \approx 5$ calculated there. It should be noted that, in contrast to the high-temperature limit, the logarithmic term arises here due to phase fluctuations. These considerations demonstrate that in a 2D superconductor the Bragg-chain model with chains along the main principal axis presents a good approximation in a broad range around the NSC MF transition.

For the essentially 3D electronic band structure under study here the characteristic interlayer Josephson tunneling amplitude η is much larger than the minimal intralayer shear stiffness $4\lambda^2 \sim 10^{-2}$, characterizing the main principal axis x in the vortex lattice. Under this condition the low-energy fluctuations of $\Delta(\mathbf{r})$ correspond to collectively sliding chains of vortices in different layers, such that the corresponding fluctuating magnetic flux lines remain nearly parallel to the external magnetic flux. Thus, similar to the situation in a 2D superconductor,[13] one may argue that these low-lying shear fluctuations determine the vortex-lattice melting point to be well below the MF H_{c2}.

For magnetic fields H above this melting point the second-order terms in λ in Eq. (4), which oscillate as function of the phases $\varphi_{n,\zeta}$, are averaged to zero by the integrations over $\varphi_{n,\zeta}$. The first-order terms in λ may also be ignored since they effectively yield only a small additive correction to β, so that their influence on the critical behavior is not important.[21] Thus, the effective free-energy functional $F_{\rm GL}$ can be written in the very simple, independent-vortex-chain form $F_{\rm GL} = \sqrt{N}\Sigma_n f_{\rm GL}^n$ with

$$f_{\rm GL}^n = \frac{a_x}{\sqrt{2\pi}} \sum_\zeta \left\{ -\alpha |c_{n,\zeta}|^2 + \frac{\beta}{2^{3/2}} |c_{n,\zeta}|^4 + \eta |c_{n,\zeta+1} - c_{n,\zeta}|^2 \right\}, \tag{5}$$

which may be considered as an effective GL energy functional for a single vortex line.

The calculation of the corresponding partition function is rather straightforward. The phase variables, $\varphi_{n,\zeta}$, can be readily integrated out. The resulting expression can be written as a functional integral over the squared amplitude $y_\zeta \equiv (\beta a_x / 2k_B T\sqrt{\pi})^{1/2} |c_\zeta|^2$, with an effective GL functional incorporating phase fluctuations

$$f_{\rm GL,eff} = k_B T \sum_\zeta \left(-\sqrt{2} x y_\zeta + \frac{1}{2} y_\zeta^2 + 2\kappa y_\zeta - \ln I_0 (2\kappa \sqrt{y_\zeta y_{\zeta+1}}) \right),$$

$$x \equiv \frac{\alpha}{\sqrt{2\beta\beta_a k_B T}} = \sqrt{\frac{\varepsilon}{\beta_a}}, \quad \kappa \equiv \frac{\eta}{\sqrt{\beta\beta_a k_B T}}, \tag{6}$$

with $\beta_a \equiv (\sqrt{\pi}/a_x)$. Here and below, for the sake of notation simplicity, we drop the vortex-chain indices.

We can then estimate the partition function in two limiting situations, for weak ($\kappa \ll 1$) and strong ($\kappa \gg 1$) interlayer coupling. In the former limit the integrals over the amplitudes can be calculated explicitly with the well-known result.[13,21] It is convenient to define the partition function per single vortex per layer, $\mathcal{Z}_v \equiv \mathcal{Z}^{1/\mathcal{N}}$, ($\mathcal{N} = NN_z$), which is given by

$$\ln \frac{\mathcal{Z}_v}{\mathcal{Z}_0} = x^2 + \ln \operatorname{erfc}(-x), \tag{7}$$

where $\operatorname{erfc}(x) \equiv (2/\sqrt{\pi}) \int_x^\infty e^{-y^2} dy$. For strong interlayer coupling the result is obtained by using the steepest descend integration, leading to

$$\ln \frac{\mathcal{Z}_v}{\mathcal{Z}_0'} = \sqrt{2} x y_0 - \frac{1}{2} y_0^2 - \frac{1}{2} \ln(4\pi\kappa) - \ln \frac{(x^2+1)^{1/4} + \sqrt{(x^2+1)^{1/2} + 2^{1/2}\kappa}}{2^{3/4}}, \tag{8}$$

where $y_0 = (x + \sqrt{x^2+1})/\sqrt{2}$. In Eqs. (7) and (8) $\mathcal{Z}_0$ and $\mathcal{Z}_0'$ are constants (i.e., independent of both x and κ), and so are thermodynamically not important.

Thus, in the liquid state above the vortex-lattice melting point one can readily derive simple limiting expressions for the spatially averaged mean-square order parameter $\langle \overline{|\Delta|^2} \rangle \equiv \int d^3 r \langle |\Delta(\vec{r})|^2 \rangle / (\mathcal{N} v)$, in the general form

$$\langle \overline{|\Delta|^2} \rangle = \frac{k_B T}{\mathcal{N}} \frac{\partial \ln \mathcal{Z}}{\partial \alpha} = \sqrt{\frac{k_B T}{2\beta\beta_a}} \left(\frac{\partial \ln \mathcal{Z}_v}{\partial x} \right) \equiv \alpha_{0I} \Phi_0(x, \kappa), \tag{9}$$

where $\alpha_{0I} = \sqrt{k_B T/(2\beta\beta_a)}$. The function $\Phi_0(x,\kappa) \equiv (\partial \ln \mathcal{Z}_v / \partial x)$ is a generalization of the universal function derived in our previous work to describe 2D superconductors, i.e.,[24,13]

$$\Phi_0(x,0) = 2[x + \exp(-x^2)/\sqrt{\pi} \operatorname{erfc}(-x)] \tag{10}$$

to the present 3D case of coupled SC layers. It is plotted in Fig. 1 for $\kappa = 0$ and $\kappa = 100$. With increasing interlayer coupling the mean-square order parameter at the MF transition point decreases within the small interval $0 \leqslant \kappa \leqslant 1$, then saturating at a nonvanishing value in the entire region $\kappa > 1$.

In Fig. 1 we also compare our result in the strong interlayer coupling limit, $\kappa = 100$, with the corresponding result obtained in the 3D Monte Carlo simulation of Sasik and Stroud.[25] The good agreement with numerical simulation and

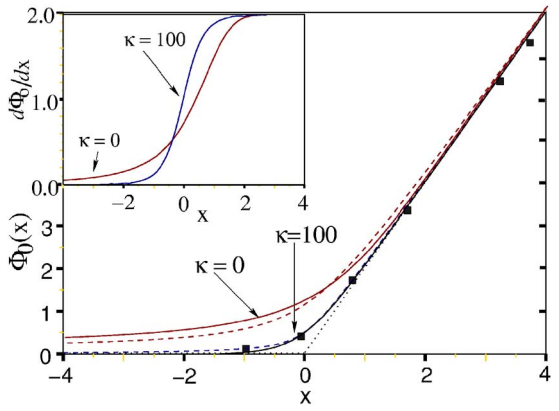

FIG. 1. (Color online) The spatially averaged mean-squared order parameter (measured in units of the 2D smearing parameter α_{0l}) $\Phi_0(x)$ as a function of the dimensionless parameter $x=\alpha/\sqrt{2\beta\beta_a k_B T}$ (see text) around the mean-field (MF) transition point $x=0$ in the weak- and strong-coupling limits (solid lines). Dashed lines represent the corresponding results calculated from a simple interpolation formula (13). The result of 3D Monte Carlo simulation by Sasik and Stroud (Ref. 25) is shown as bold squares. The dotted straight line represents the result of mean-field theory. Inset: The derivative with respect to x is plotted to emphasize the region where SC fluctuations are strong. Note the gross similarity between the two limiting curves within the main crossover region around the MF H_{c2}.

optimized perturbation theory[9] provides strong support for the validity of the extension of our Bragg-chain model to 3D superconductors.

It is easy to show, by means of Eq. (8), that for $\kappa \gg 1$ the function $\Phi_0(x \to 0, \kappa) \to 1/2$, irrespective of κ. The universal nonvanishing value of $\langle|\overline{\Delta}|^2\rangle$ at the MF transition point in the strong interlayer-coupling limit reflects a significant smearing of the SC phase transition due to thermal fluctuations. This effect characterizes the GL theory of a 3D superconductor at high magnetic fields, since above the vortex-lattice melting point it can be mapped to the GL theory of a 1D superconductor at zero magnetic field, where a genuine phase transition is absent.[26] In the zero-coupling limit $\eta \to 0$, the effective GL free-energy functional in a given SC layer, appearing within the curly brackets in Eq. (5), is equivalent to the GL energy functional for a 0D superconductor near the SC transition at vanishing magnetic field[27]

$$f_{\mathrm{GL}}^{(0)}(|\psi|^2) = k_B T_{c0}\left[\frac{1}{\delta}(t-1)|\psi|^2 + \frac{0.106}{\delta}|\psi|^4\right].$$

Here, $T_{c0}=T_c(H=0)$, $t=T/T_{c0}$, and $\delta=[N(0)v k_B T_{c0}]^{-1}$ is the quantum-size parameter of the SC grain [$N(0)$ is the electronic density of states per unit volume at the Fermi energy and v is the volume of the small SC particle]. The corresponding MF free energy is

$$\tilde{f}_{\mathrm{GL}}^{(0)}(T, H \to 0) = -4.7 k_B T_{c0}(1-t)^2/\delta.$$

For the isolated SC layer at high magnetic field and low temperature $T \ll T_{c0}$ it was found that $\alpha \approx (1-h)/4\hbar\omega_c$, with $h \equiv H/H_{c2}(T \to 0)$ and $\beta \approx 1.38/(\hbar\omega_c)^2 E_F$.[13] Here, $\omega_c = eH/m^* c$ is the cyclotron frequency with m^* the in-plane effective cyclotron mass and E_F the Fermi energy. The corresponding MF free energy is

$$\tilde{f}_{\mathrm{GL}}^{(0)}(T \to 0, H) \approx -E_F(1-h)^2/16\beta_a.$$

For general T and H values near the MF transition line, $H_{c2}(T)=\phi_0/2\pi\xi(T)^2=H_{c2}(0)(1-T/T_{c0})$, the simple weak-coupling BCS theory yields a single scaling formula for the MF free energy

$$\tilde{f}_{\mathrm{GL}}^{(0)}(T,H) = \tilde{f}_{\mathrm{GL}}^{(0)}(0,0)(1-\tau)^2 = \tilde{f}_{\mathrm{GL}}^{(0)}(0,0)(1-T/T_{c0})^2[1-H/H_{c2}(T)]^2, \quad (11)$$

where $\tau=t+h$, so that by equating the coefficient $\tilde{f}_{\mathrm{GL}}^{(0)}(0,0)$ in the two limiting regions of the phase boundary, i.e., $\tilde{f}_{\mathrm{GL}}^{(0)}(0,0)=4.7k_B T_{c0}/\delta=E_F/16\beta_a$, with $\beta_a \approx 1$, one finds $\delta=77k_B T_{c0}/E_F$.

Using the well-known BCS expression for the zero-temperature coherence length $\xi(0)=0.18\hbar v_F/k_B T_{c0}$, we find that

$$\delta \approx \left(\frac{28}{k_F \xi(0)}\right). \quad (12)$$

This enables us to estimate the effective spatial size of the SC grain in the equivalent zero magnetic-field problem. Since our original model system consists of a 2D SC layer, the effective grain volume is an area $v \equiv a^2$, and the DOS function is that of a 2D electron gas, $N(0)=m^*/2\pi\hbar^2=k_F^2/4\pi E_F$, so that $\delta \approx 35[\xi(0)/a](1/k_F a)$. Comparing this expression to Eq. (12), we find that the radius of the effective SC grain $a \sim \xi(0)$, which is approximately equal to $a_{H_{c2}(0)}$, the smallest length scale in a 2D SC condensate under a perpendicular magnetic field $H \approx H_{c2}(0)$. For MgB_2 we have $T_{c0} \approx 40$ K and $E_F/k_B \approx 13\,000$ K, so that $\delta=0.23$. Similarly, for YNi_2B_2C with $T_{c0} \approx 15.5$ K and $E_F/k_B \approx 1750$ K, we find $\delta=0.675$.

These results show that a single SC layer in a high magnetic field above the vortex-lattice melting point is equivalent to a 0D superconductor at zero magnetic field.[27] The coupled-layer model is therefore equivalent to a 1D Josephson array of small SC grains, discussed, e.g., in Refs. 27 and 28. For the relatively large effective quantum-size parameters $\delta=0.23$ and 0.675, estimated above, the numerical simulations reported in Ref. 27 show that the reduction of the transition width by the interlayer coupling is not very significant.

In what follows we shall provide an analytical argument in support of this remarkably weak influence of the interlayer coupling constant. To simplify the analysis let us approximate the function $\Phi_0(x,\kappa)$ by means of an interpolation formula, suggested by Ito *et al.*[7] in fitting their experimental dHvA data for a quasi-2D organic superconductor, namely,

$$\Phi_{0,\mathrm{interp}}(x,\kappa) = x + \sqrt{\nu_\kappa^2 + x^2}, \quad (13)$$

where the fitting parameter ν_κ depends only on the interlayer coupling. The equivalence of Eq. (13) to the interpolation formula presented in Ref. 7 is made clear if we note that

from Eq. (6) $x=\alpha/2\beta\beta_a\alpha_{0I}\approx[1-H/H_{c2}(T)]\Delta_0^2/2\alpha_{0I}$, where Δ_0 is the amplitude of the SC order parameter at $T=0$ and $H=0$.

The best fitting function $\Phi_{0,\text{interp}}(x,\kappa)$ is represented in Fig. 1 by the dashed lines for the limiting cases $\kappa=0$ and $\kappa \gg 1$. At zero interlayer coupling the parameter ν_κ can be obtained by comparing $\Phi_{0,\text{interp}}(x,0)$ with $\Phi_0(x,0)$ given by Eq. (10). This yields $\nu_{\kappa=0}=2/\sqrt{\pi}\approx 1.13$. In the strong-coupling limit the best fit is obtained for $\nu_{\kappa=100}=0.51$.

Thus, the actual smearing parameter $\alpha_I=\nu_\kappa\alpha_{0I}$ changes quite moderately, i.e., with ν_κ in the relatively small region

$$\nu_\kappa \approx 0.51 - 1.13,$$

when the coupling constant κ varies between $\kappa=0$ and $\kappa \gg 1$, i.e., in the entire range between 2D and 3D systems. This result is universal, i.e., independent of the microscopic parameters k_F and $\xi(0)$, which determine the quantum-size parameter δ [see Eq. (12) and note the close relation to the Ginzburg critical region].

The parameter $\alpha_I=\nu_\kappa\sqrt{k_BT/2\beta\beta_a}$, which controls the smearing of the phase transition by fluctuations, is related to the parameter α_F introduced in Ref. 14 (denoted there by α) by $\alpha_F=2\alpha_I/\Delta_0^2$, where Δ_0 is identified with the effective zero-field energy gap $\Delta_E(0)$ of Ref. 14. Using the above value of β, obtained from the 2D electron gas model, we find

$$\alpha_I \approx 0.35\nu_\kappa \hbar\,\omega_c\sqrt{E_F k_B T}, \tag{14}$$

which reflects the smearing effects due to the magnetic field and temperature and the narrowing of the crossover region by the interlayer coupling parameter κ.

We now compare the theoretical results with experimental data we obtained for YNi_2B_2C. The investigated single crystal was grown by a flux technique as described elsewhere.[29] The dHvA effect was measured utilizing a cantilever torque technique in a ^{3}He cryostat equipped with a 15 T superconducting magnet. The sample could be rotated in situ around one axis. The torque signal for the magnetic field aligned 8° away from the c axis towards the a axis is shown in Fig. 2.

Below about 8 T, a pronounced hysteresis with an extraordinary strong peak effect is observed. This peak effect, well known for a number of other type-II superconductors and interesting by itself,[30] is unwanted here since it hampers the reliable extraction of dHvA oscillations in this range. Above and below the peak-effect region, however, the dHvA signal can be resolved as visualized in the insets of Fig. 2 where a background signal (fitted by a low-order polynomial) has been subtracted. The dHvA oscillations persist down to about 6.3 T, clearly within the hysteretic region. This is somewhat different to the strong damping found for other YNi_2B_2C single crystals grown by the zone-melting method.[31] This adds to the quite controversial results reported for the dHvA-signal damping in YNi_2B_2C.[32–34] In the peak-effect region no oscillations can be extracted, but at lower fields, deep in the superconducting region (down to 3 T), quite strong dHvA oscillations with the same frequency as in the normal state are detected (left inset in Fig. 2). Although this is a remarkable observation the low-field dHvA signal will not be considered further here.

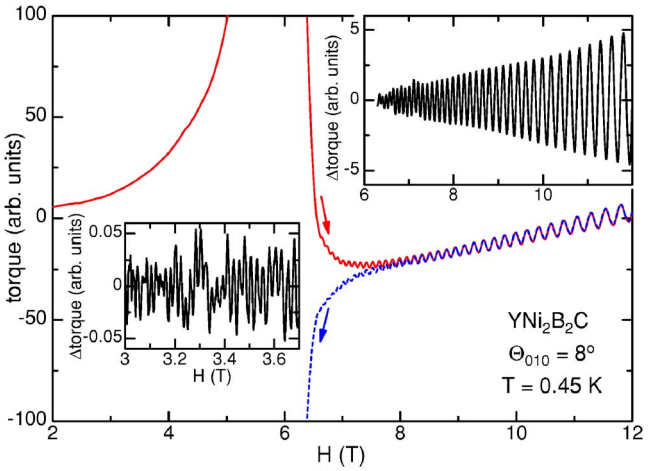

FIG. 2. (Color online) Field dependence of the torque signal of a flux-grown YNi_2B_2C single crystal with the magnetic field rotated by 8° from the c axis towards the a axis. The arrows indicate the field-sweep direction. The insets show the oscillating torque signal after background subtraction.

We have fit the additional damping of the dHvA oscillations in the vortex state above the peak-effect region using the random-vortex-lattice model described in Ref. 13 [Fig. 3(a)]. We have as well exploited the vortex-chain flow model[24] to calculate the magnetic-field dependence of the magnetization difference ΔM between the two branches of the hysteresis loop shown in Fig. 2. In Ref. 24 it was shown that ΔM is proportional to the function $\Phi_0(x,\kappa)$ defined in Eq. (9). This has been done by using the interpolation formula (13) with $\alpha_{0I}=\alpha_I/\nu_\kappa$ and α_I given by Eq. (14) with $\nu_\kappa=0.5$, corresponding to the 3D limit.

Treating the zero-field amplitude Δ_0 of the SC order parameter and the MF H_{c2}, as adjustable parameters, the best fit for both data sets shown in Fig. 3 is obtained for $\Delta_0\simeq 7.6$ meV and $H_{c2}\simeq 6.8$ T. Here, the experimentally determined values for the cyclotron effective mass $m^*/m_e \approx 0.4$ and the Fermi energy corresponding to the detected cross-sectional area, i.e., $E_F/k_B=\hbar\,\omega_c F/(k_B H)=1750$ K with $F=520$ T, together with the temperature $T=0.45$ K have been used. Thus, a single set of parameters yields a good agreement with data extracted from the steady and oscillating parts of the magnetization. The resulting dimensionless smearing parameter is found to take the value $\alpha_F\approx 0.033$. Note, however, that the obtained amplitude of the order parameter Δ_0 is significantly larger than the $T=0$, $H=0$ SC gap parameter of ≈ 2 meV found for this material from tunneling data and photoemission spectroscopy[35–38] (see the discussion below).

We further compare our theory with available experimental data for MgB_2. With the parameters reported by Fletcher *et al.*,[14] i.e., with $m^*\approx 0.3m_e$, $\Delta_0=17$ meV, $F=2930$ T, measured at $T=0.32$ K, so that $E_F/k_B=13\,000$ K, our theoretical estimate is $\alpha_I\approx 479$ K^2 or $\alpha_F\approx 0.024$. This result is similar to, but somewhat smaller than the best fitting value of $\alpha_F \approx 0.055$ obtained in Ref. 14.

Again, it is interesting to note that, similar to the situation described above for YNi_2B_2C, in the fitting procedure em-

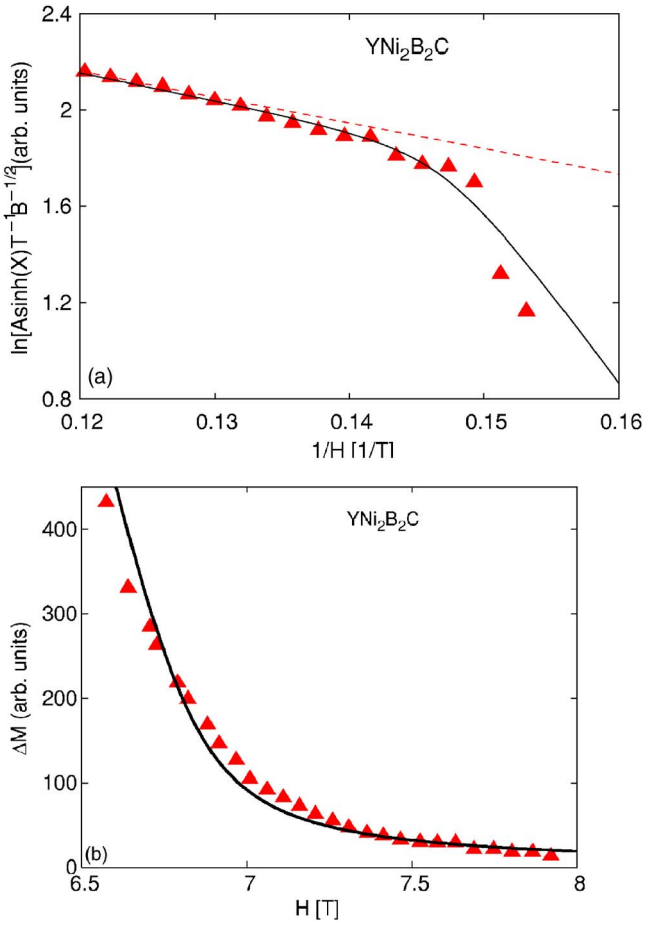

FIG. 3. (Color online) (a) Dingle plot of the dHvA signal shown in Fig. 2 close to the SC transition (solid line) and the extrapolation of the corresponding Dingle plot from the normal state (dashed line). (b) Magnetization difference between the up and down sweep of the hysteresis loop shown in Fig. 2. Full triangles show the experimental data, while the solid lines represent best fits as described in the text. Both theoretical curves were obtained for $\Delta_0 \simeq 7.6$ meV and $H_{c2} \simeq 6.8$ T.

ployed in Ref. 14, Δ_0 was found significantly larger than the zero-field SC gap parameter Δ_π derived from tunneling experiments. Both discrepancies seem to have the same origin, which is associated with the breakdown of the universal scaling behavior of the SC free energy along the entire NSC phase boundary of the studied materials. This scaling law [see Eq. (11)] connects the low-temperature sector of the MF transition line, determined by $\Delta_0/\hbar\omega_c \approx 0.61\sqrt{E_F/\hbar\omega_c}$,[13] to the high-temperature sector, determined by the BCS relation $\Delta_0 = 1.76 k_B T_{c0}$, when the latter is substituted into the following equivalent form of the former:

$$H_{c2}[\text{in T}] = \frac{1}{2}\left(\frac{\Delta_0}{1.76 k_B T_{c0}}\right)^2 \left(\frac{a_{H=1\ \text{T}}}{\xi(0)}\right)^2. \qquad (15)$$

Here $a_{H=1\ \text{T}}$ ($\approx$256 Å) is the magnetic length at $H=1$ T. For both materials this scaling-law is badly violated. In YNi_2B_2C the BCS relation, which yields $\Delta_0 = 2.43$ meV, agrees rather well with the zero-field tunneling data, but when inserted into Eq. (15) yields a value for the low-temperature H_{c2} ($\approx$0.34 T) which is more than an order of magnitude smaller than what is actually observed. Similarly, in MgB_2, the BCS relation yields $\Delta_0 = 6.07$ meV, which is consistent with the SC gap extracted from tunneling experiment, whereas when combining it with Eq. (15) leads to the very small value $H_{c2}(0) \approx 0.21$ T. In contrast, the values of Δ_0 extracted from the above fittings, when substituted in Eq. (15), yield $H_{c2}(0) \approx 3.3$ T, and $H_{c2}(0) \approx 1.7$ T, for YNi_2B_2C and MgB_2, respectively, which are in much better agreement with the measured values.

In conclusion, it was shown here that the transition to the low-temperature SC state in a pure, strongly type-II, 3D layered superconductor is smeared by the magnetic field in magnitude comparable to that expected for 2D superconductors. The predicted weak dependence of the smearing on the interlayer coupling is found to be universal, i.e., independent of the microscopic parameters determining the Ginzburg critical region. As shown clearly in Fig. 1, large ratios of the 2D fluctuation effect to the corresponding effect in 3D are found only in the region well above the MF H_{c2}, where the fluctuations are relatively small in both systems. The theoretically predicted width of the transition region is found to be in good agreement with experimental data of the dHvA effect in the SC state of both YNi_2B_2C and MgB_2.

This research was supported by a grant from the Israel Science Foundation founded by the Academy of Sciences and Humanities and by the fund from the promotion of research at the Technion. The work at Dresden was supported by the DFG through SFB463. Ames Laboratory is operated for the U. S. Department of Energy by Iowa State University under Contract No. W-7405-Eng-82.

[1] P. H. Kes, C. J. van der Beek, M. P. Maley, M. E. McHenry, D. A. Huse, M. J. V. Menken, and A. A. Menovsky, Phys. Rev. Lett. **67**, 2383 (1991).
[2] N. K. Wilkin and M. A. Moore, Phys. Rev. B **48**, 3464 (1993).
[3] D. Li and B. Rosenstein, Phys. Rev. B **65**, 220504(R) (2002).
[4] P. A. Lee and S. R. Shenoy, Phys. Rev. Lett. **28**, 1025 (1972).
[5] J. S. Urbach, W. R. White, M. R. Beasley, and A. Kapitulnik, Phys. Rev. Lett. **69**, 2407 (1992).
[6] T. Sasaki, T. Fukuda, N. Yoneyama, and N. Kobayashi, Phys. Rev. B **67**, 144521 (2003).
[7] H. Ito, S. M. Hayden, P. J. Meeson, M. Springford, and G. Saito, J. Supercond. **12** 525 (1999).
[8] Z. Tesanovic and A. V. Andreev, Phys. Rev. B **49**, 4064 (1994); Z. Tesanovic, L. Xing, L. Bulaevskii, Q. Li, and M. Suenaga, Phys. Rev. Lett. **69**, 3563 (1992).
[9] D. Li and B. Rosenstein, Phys. Rev. B **65**, 024513 (2001); **65**, 024514 (2001).
[10] D. Li and B. Rosenstein, Phys. Rev. Lett. **86**, 3618 (2001).

[11] D. Li and B. Rosenstein, Phys. Rev. B **70**, 144521 (2004).
[12] V. Zhuravlev and T. Maniv, Phys. Rev. B **60**, 4277 (1999).
[13] T. Maniv, V. N. Zhuravlev, I. D. Vagner, and P. Wyder, Rev. Mod. Phys. **73**, 867 (2001).
[14] J. D. Fletcher, A. Carrington, S. M. Kazakov, and J. Karpinski, Phys. Rev. B **70**, 144501 (2004).
[15] T. Isshiki, H. Maruyama, N. Kimura, T. Nojima, A. Ochiai, and H. Aoki, Physica C **417**, 110 (2005).
[16] G. J. Ruggeri and D. J. Thouless, J. Phys. F: Met. Phys. **6**, 2063 (1976).
[17] E. Brezin, A. Fujita, and S. Hikami, Phys. Rev. Lett. **65**, 1949 (1990).
[18] S. Hikami, A. Fujita, and A. I. Larkin, Phys. Rev. B **44**, 10400 (1991).
[19] N. K. Wilkin and M. A. Moore, Phys. Rev. B **47**, 957 (1993).
[20] V. Zhuravlev and T. Maniv, Phys. Rev. B **66**, 014529 (2002).
[21] T. Maniv, V. N. Zhuravlev, I. D. Vagner, and P. Wyder, Physica B **315**, 47 (2002).
[22] Y. Kato and N. Nagaosa, Phys. Rev. B **48**, 7383 (1993).
[23] V. N. Zhuravlev and T. Maniv (unpublished).
[24] T. Maniv, V. Zhuravlev, J. Wosnitza, and J. Hagel, J. Phys.: Condens. Matter **16**, L429 (2004).
[25] R. Sasik and D. Stroud, Phys. Rev. Lett. **75**, 2582 (1995).
[26] L. D. Landau and E. M. Lifshitz, *Statistical Physics* (Adisson-Wesley, New York, 1958).
[27] C. Ebner and D. Stroud, Phys. Rev. B **23**, 6164 (1981).
[28] D. J. Scalapino, M. Sears, and R. A. Ferrell, Phys. Rev. B **6**, 3409 (1972).
[29] P. C. Canfield, P. L. Gammel, and D. J. Bishop, Phys. Today **51**, 40 (1998).
[30] M. Marchevsky, M. J. Higgins, and S. Bhattacharya, Nature (London) **409**, 591 (2001).
[31] O. Ignatchik, T. Coffey, J. Hagel, M. Jackel, E. Jobiliong, D. Souptel, G. Behr, and J. Wosnitza, J. Magn. Magn. Mater. **290-291**, 424 (2005).
[32] G. Goll, M. Heinecke, A. G. M. Jansen, W. Joss, L. Nguyen, E. Steep, K. Winzer, and P. Wyder, Phys. Rev. B **53**, R8871 (1996); G. Goll, L. Nguyen, E. Steep, A. G. M. Jansen, P. Wyder, and K. Winzer, Physica B **230-232**, 868 (1997).
[33] Taichi Terashima, Hiroyuki Takeya, Shinya Uji, Kazuo Kadowaki, and Haruyoshi Aoki, Solid State Commun. **96**, 459 (1995); T. Terashima, C. Haworth, H. Takeya, S. Uji, H. Aoki, and K. Kadowaki, Phys. Rev. B **56**, 5120 (1997).
[34] D. Bintley and P. J. Meeson, Physica C **388-389**, 181 (2003).
[35] P. Martinez-Samper, H. Suderow, S. Vieira, J. P. Brison, N. Luchier, P. Lejay, and P. C. Canfield, Phys. Rev. B **67**, 014526 (2003).
[36] T. Yokoya, T. Kiss, T. Watanabe, S. Shin, M. Nohara, H. Takagi, and T. Oguchi, Phys. Rev. Lett. **85**, 4952 (2000).
[37] Toshikazu Ekino, Hironobu Fujii, Makoto Kosugi, Yuji Zenitani, and Jun Akimitsu, Phys. Rev. B **53**, 5640 (1996).
[38] H. Sakata, M. Oosawa, K. Matsuba, N. Nishida, H. Takeya, and K. Hirata, Phys. Rev. Lett. **84**, 1583 (2000).